POLITECNICO DI TORINO
Repository ISTITUZIONALE

Sparse Reconstruction of Glucose Fluxes Using Continuous Glucose Monitors

(Article begins on next page)

08 November 2022

Sparse Reconstruction of Glucose Fluxes Using Continuous Glucose Monitors

Ali A. Al-Matouq   Taous-Meriem Laleg-Kirati   Carlo Novara   Ivana Rabbone   and Tyrone Vincent

Abstract—A new technique for estimating postprandial glucose flux profiles without the use of glucose tracers is proposed. A sparse vector space representation is first found for the space of plausible glucose flux profiles using sparse encoding. A Lasso formulation is then used to estimate the glucose fluxes that combines (1) known patient model parameters; (2) the vector space of plausible glucose flux profiles; (3) continuous glucose monitor measurements taken during the meal; (4) amount of insulin injected; (5) amount of meal carbohydrates; and (6) an estimate of the initial conditions. Three glucose fluxes are then estimated, namely; glucose rate of appearance from the intestine; endogenous glucose production from the liver; insulin dependent glucose utilization; and other important state variables. The simulation results show that the technique is capable of estimating the glucose fluxes with high accuracy, even for complex meal scenarios. The experimental results indicate that the technique is capable of reproducing the triple tracer measurements for three T1DM undergoing the triple tracer protocol while estimating the missing measurements for a certain model parameter selection.

Index Terms—Glucose metabolism, continuous glucose monitors, type 1 diabetes, meal tolerance test, sparse encoding, lasso estimation

1 INTRODUCTION

THE goal of artificial pancreas (AP) systems is to enable people with type 1 diabetes mellitus (T1DM) to live healthy and convenient lives without the complications of diabetes. However, mimicking the physiological pattern of insulin secretion during meals remains one of the most difficult challenges in AP system development [1], [2], [3]. One of the major reasons for this difficulty is multiple glucose interactions occurring simultaneously during meals that are currently measured using invasive techniques. Continuous glucose monitors (CGM) can only measure subcutaneous glucose concentrations in real time and has been successfully used in many recently developed AP systems for regulating nighttime glucose [2]. However, during meals, the situation gets more complicated as glucose traffic in the circulation becomes affected by the appearance of glucose from the intestine, due to the digestion of meal carbohydrates and the disappearance of glucose from plasma due to insulin activation and supression of endogenous glucose production. The premise is that for effective control of glucose during meals, it is important to measure the extent of glucose appearances and disappearances in plasma [4].

Glucose rate of appearance from the intestine, u_{ra} (mg/kg min), is the glucose flux from the intestine to plasma resulting from the digestion of meal carbohydrates (CHO) [5]. The flux profile for u_{ra} has a magnitude that depends on the size of the meal and a duration that depends on meal composition [1]. In healthy individuals, the pancreas β cells will be partially stimulated to release insulin due to the cephalic response [6] and the secretion of incretin hormones by the intestine before reaching elevated glucose levels [1]. This physiological signal acts as a natural "feedforward" signal for regulating glucose during meals. However, people with T1DM require external insulin with a dosage that is calculated and injected without access to this important physiological signal.

Another major flux is referred to as glucose utilization, u_{ins} (mg/kg · min), which measures the absorption rate of glucose by muscles and adipose tissue due to insulin activation [7]. This outlet glucose flux has a profile with a magnitude that depends primarily on the amount of insulin administred to the patient and insulin sensitivity at the time of the meal, which can vary considerably depending on the condition of the patient, time of the day etc. [3]. Yet another glucose flux is glucose production from the liver, $u_{egp}(t)$ (mg/kg · min), which is high when fasting and normally suppressed by meal insulin. Other secondary outlet glucose fluxes are insulin independent glucose utilization by brain and erythrocytes, u_{ii} (mg/kg · min), and renal excretion of glucose in urine, u_e (mg/kg · min) during relatively high glucose concentrations [7].

The three main glucose fluxes, namely; u_{ra}, u_{egp} and u_{ins} can be estimated in a clinical setting using multiple injected tracers while a patient is undergoing a meal tolerance test

- A. A. Al-Matouq is with the Faculty of Engineering Management, Prince Sultan University, PO Box 66863 Rafha Street, Riyadh 11586, Saudi Arabia. E-mail: almatouq@psu.edu.sa.
- T.-M. Laleg-Kirati is with the Computer, Electrical and Mathematical Science and Engineering (CEMSE) Division, King Abdullah University of Science and Technology, Thuwal 23955-6900, Saudi Arabia. E-mail: taousmeriem.laleg@kaust.edu.sa.
- C. Novara is with the Politecnico di Torino, Turin 10129, Italy. E-mail: carlo.novara@polito.it.
- I. Rabbone is with SSD Diabetologia Endocrinologia Pediatrica Ospedale Infantile Regina Margherita, AOU Citt della Salute e della Scienza di Torino, University of Turin, Torino 10124, Italy. E-mail: ivana.rabbone@unito.it.
- T. Vincent is with the Department of Electrical Engineering and Computer Science, Colorado School of Mines 1600 Illinois St., Golden, CO 80401. E-mail: tvincent@mines.edu.

TABLE 1
Nomenclature

| Variable	Description	Unit
g	plasma glucose concentration	mg/dl
g_p	mass of glucose in plasma	mg/kg
g_t	mass of glucose in tissue	mg/kg
g_{sc}	mass of subcutaneous glucose	mg/kg
u_{ra}	glucose rate of appearance from intestine	mg/kg min
u_{egp}	endogenous glucose production	mg/kg min
u_{ins}	insulin dependent glucose utilization	mg/kg min
u_{ii}	insulin independent glucose utilization	mg/kg min
u_e	renal excretion	mg/kg min
i	plasma insulin concentration	pmol/l
i_p	mass of insulin in plasma	pmol/kg
i_l	mass of insulin in liver	pmol/kg
u_{ira}	insulin rate of appearance	pmol/kg min
i_{sc1}	insulin mass in 1st subcutaneous compart.	pmol/kg
i_{sc1}	insulin mass in 2nd subcutaneous compart.	pmol/kg
i_{d1}	insulin action on glucose production	pmol/l
i_{d2}	delayed compartment for insulin action	pmol/l
u_{iir}	insulin infusion rate	pmol/kg min
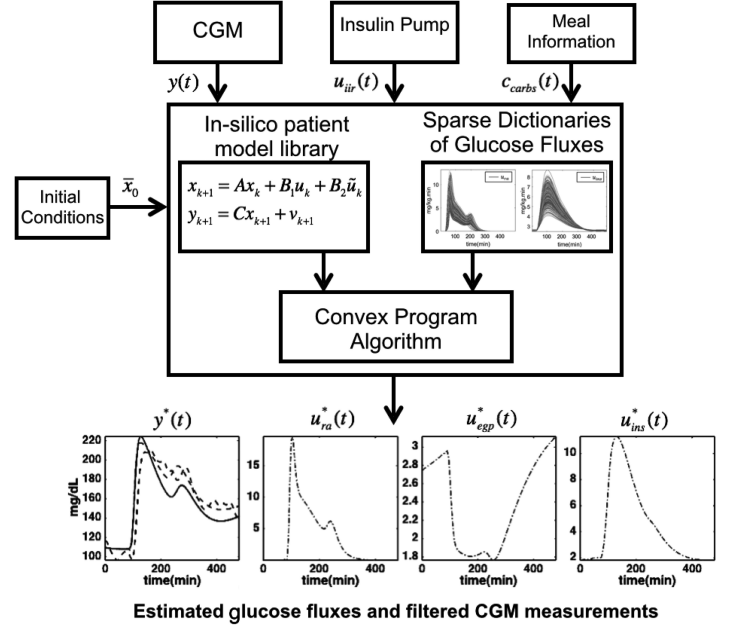
Fig. 1. Proposed framework for postprondial estimation of glucose fluxes.

(MTT) [8]. Such complex protocols, however, are expensive, invasive and can be subject to substantial errors as noted in [8]. In the triple tracer technique developed in [9], for example, two tracers are infused intravenously using infusion patterns that mimic typical patterns of u_{egp} and u_{ra} while the third tracer is mixed with the meal. Five different plasma glucose measurements are then taken to trace back the different labelled and unlabelled glucose concentrations assuming the one compartment Steele's model [10] or the two compartment Radziuk/Mari model [11]. Attempts to reduce estimation errors of the dual tracer technique was made in [12], under the framework of maximum likelihood estimation and recently in [13] under the Baysian estimation framework.

An attempt for estimating u_{ra} without the use of tracers and with minimal patient parameter identification was made in [14]. Bergman's minimal model in [15] was used, assuming model parameters at average values except for patient specific insulin sensitivity which was found using numerical calculations. The technique, however, still requires intravenous measurements of both plasma glucose and plasma insulin and can only estimate u_{ra} assuming no measurement noise present. In [16], an algorithm was developed that uses the difference between predictions from a simple glucose-insulin model and CGM measurements to detect meal occurrences and to concurrently estimate u_{ra}. A recent study in [17] phrased the problem of identifying glucose fluxes as a blind identification problem for identifying both model parameters and unmeasured disturbances simultaneously from CGM and insulin pump measurements.

In this study, a different approach will be used for estimating the three main glucose fluxes without the use of tracers. Sparse encoding will be exploited to discover the building blocks for the space of plausible glucose flux profiles, for both u_{ra} and u_{ins} during meals using a training set obtained from random simulations of the UVa Padova model [18]. The constructed sparse dictionaries (basis vectors) will be then used to find the best combination of basis vectors that explain CGM glucose measurements and insulin infusion recordings while being consistent with a known glucose/insulin transport model for the patient. This will be done by casting the estimation problem as a Lasso problem (least absolute shrinkage and selection operator) [19] that combines both the known parameters of the UVa Padova model and the glucose flux

basis vectors in one formulation. Fig. 1 shows a block diagram describing the proposed estimation framework.

To verify the technique, the study first demonstrates, in simulation, that sparse basis vectors originally constructed using sparse encoding of a certain training set, can be used to sparsely represent flux profiles beyond the training set. Furthermore, our simulation results demonstrate that the method can estimate the glucose fluxes with high accuracy even in the presence of complex CGM measurement noise and under scenarios involving multiple meal stages and insulin injections. Finally, the method was tested and verified on data for 3 T1DM patients undergoing the triple tracer protocol while coupled to CGM devices. Our results show that the method is capable of reproducing most of the measurements obtained from the triple tracer technique patients using a certain selection of patient model parameters. This was achieved despite using the same sparse basis vectors for representing u_{ra} and u_{ins} fluxes in all experiments. The technique, however, assumes knowledge of patient parameters relevant to the transport model used which may be difficult to obtain in practice without triple tracer experiments. Also, the method requires the availability of a representative set of plausible glucose flux profiles for the patient (or set of patients). The study assumes that the UVa Padova simulator can be used for generating plausible glucose flux profiles for the patient and that patient parameters are known in advance.

The following is the outline of this study. Section 2 will reintroduce the transport equations for plasma glucose, plasma insulin and endogenous glucose production subsystems as given in [7]. Section 3 will give the problem formulation used to estimate the glucose fluxes along with the required assumptions. Section 4 will present the simulation experiments conducted to find the vector space of plausible glucose flux profiles. Section 5 will present the simulation results and finally Section 6 will provide the experimental study. The following notation is used in this study: $\mathbb{R}$ represents the set of real numbers; $A \in \mathbb{R}^{m \times n}$ is an $m \times n$ matrix with real values; $\|z\|_{l_i}$ is the ℓ_i norm of vector z while $|z|$ is the number of non-zero elements in z. Table 1 provides the nomenclature used in this study.

2 TRANSPORT MODEL EQUATIONS

In this study, the transport model for the glucose/insulin control system given in [18] will be partially adapted. In the following, a review of the linear subsystem equations for the glucose, insulin and endogenous glucose production will be briefly given to demonstrate the formation of the state space representation and the notation used in this study.

2.1 Glucose Subsystem

The glucose subsystem transport model in the UVA/Padova model [18] is given by the following:

$$
\begin{aligned}
\frac{dg_p(t)}{dt} &= u_{ra}(t) + u_{egp}(t) - u_{ii}(t) - u_e(t) - k_1 g_p(t) + k_2 g_t(t), \\
\frac{dg_t(t)}{dt} &= -u_{ins}(t) + k_1 g_p(t) - k_2 g_t(t), \\
\frac{dg_{sc}(t)}{dt} &= \frac{1}{\tau}(g(t) - g_{sc}(t)), \\
g(t) &= g_p(t)/v_g, \\
g_p(0) &= g_{pb}, \quad g_t(0) = g_{tb}, \quad g_{sc}(0) = \frac{g_{pb}}{v_g},
\end{aligned}
\tag{1}
$$

where $g_p(t)$ (mg/kg) is mass of glucose in plasma and fast equilibrating tissue per kg of patient body weight; $g_t(t)$ (mg/kg) is mass of glucose in slowly equilibrating tissue per kg of patient body weight; $g(t)$ is plasma glucose concentration in (mg/dl) and $g_{sc}(t)$ is subcutaneous glucose concentration in mg/dl. The glucose fluxes are in units of mg per kg patient body weight per minute, i.e., (mg/kg min) and are the glucose rate of appearance from the intestine $u_{ra}(t)$, the endogenous glucose production from the liver $u_{egp}(t)$, the renal excretion of glucose in urine $u_e(t)$, the insulin independent glucose utilization by brain cells and erythrocytes $u_{ii}(t)$ and the insulin dependent glucose utilization by muscle and adipose tissue $u_{ins}(t)$. Here, v_g is the distribution volume of glucose in plasma in (dl/kg) and k_1 and k_2 in min^{-1} are the diffusion rates of glucose between plasma and peripheral tissue and peripheral tissue to plasma, respectively. The initial conditions for the states are given by the basal levels of plasma glucose g_{pb} and tissue glucose g_{tb}, respectively. Finally, τ(min) is a time lag accounting for both physiological and sensor delays.

2.2 Insulin Subsystem

Insulin kinetics in [18] is described using a two compartment model as follows:

$$
\begin{aligned}
\frac{di_p(t)}{dt} &= -(m_2 + m_4)i_p(t) + m_1 i_l(t) + u_{ira}(t) \\
\frac{di_l(t)}{dt} &= m_2 i_p(t) - (m_1 + m_3)i_l(t) \\
i(t) &= i_p(t)/v_i, \quad i_p(0) = i_{pb}, \quad i_l(0) = i_{lb},
\end{aligned}
\tag{2}
$$

where $i_p(t), i_l(t)$ (pmol/kg) are insulin masses in plasma and liver respectively; $i(t)$ pmol/l is plasma insulin concentration; u_{ira} (pmol/kg min) is insulin rate of appearance in plasma; v_i (l/kg) is the distribution volume of insulin; m_1, m_2(min^{-1}) are the diffusion rates of insulin from liver to plasma and from plasma to liver respectively while m_3 and m_4 (min^{-1}) are rates of liver and peripheral insulin degradation respectively (assumed linear). The initial conditions for

the two states are given by the basal levels of plasma insulin i_{pb} and liver insulin i_{lb} respectively. Insulin rate of appearance is described by the following two compartment model:

$$
\begin{aligned}
\frac{di_{sc1}(t)}{dt} &= -(k_d + k_{a1})i_{sc1}(t) + u_{iir}(t), \quad i_{sc1}(0) = i_{sc1ss} \\
\frac{di_{sc2}(t)}{dt} &= k_d i_{sc1}(t) - k_{a2} i_{sc2}(t) \\
u_{ira}(t) &= k_{a1} i_{sc1}(t) + k_{a2} i_{sc2}(t), \quad i_{sc2}(0) = i_{sc2ss},
\end{aligned}
\tag{3}
$$

where $i_{sc1}(t), i_{sc2}(t)$ (pmol/kg) are insulin masses in the first and second subcutaneous compartments, $u_{iir}(t)$ (pmol/kg min) is the subcutaneous insulin infusion rate while k_{a1}, k_{a2} (min^{-1}) and k_d(min^{-1}) are rate parameters.

2.3 Endogenous Glucose Production Subsystem

Endogenous glucose production is described by:

$$
\begin{aligned}
\frac{di_{d1}}{dt} &= -k_i(i_{d1}(t) - i_{d2}(t)) \\
\frac{di_{d2}}{dt} &= -k_i(i_{d2}(t) - i(t)) \\
u_{egp} &= k_{p1} - k_{p2} g_p(t) - k_{p3} i_{d1}(t) \\
i_{d1}(0) &= i_{d2}(0) = i_{pb}/v_i,
\end{aligned}
\tag{4}
$$

where $i_{d1}(t)$ (pmol/l) is called insulin action on glucose production; $i_{d2}(t)$ (pmol/l) is the delayed compartment for insulin action; k_{p1}(mg/kg min) is the extrapolated endogenous glucose production at zero glucose and insulin, k_{p2}(min^{-1}) is liver glucose effectiveness, k_{p3}(mg/kg min per pmol/l) is a parameter governing amplitude of insulin action on the liver and k_i(min^{-1}) is a rate parameter accounting for delay between insulin signal and insulin action.

Assumption 2.1. *Initially no meal carbohydrates are on board; i.e., $u_{ra}(0) = 0$. Furthermore, as in [18], $u_{ii} = u_{cns} = 1 \text{ mg/kg} \cdot \text{min}$ while $u_e \approx 0$ i.e., no renal excretion of glucose in urine.*

The system of Equations (1), (3), and (4) forms a linear time invariant system which can be represented in standard state space form as:

$$
\begin{aligned}
\dot{x}(t) &= A_c x(t) + B_{c,1} u(t) + B_{c,2} \tilde{u}(t) \\
y(t) &= C_c x(t),
\end{aligned}
\tag{5}
$$

where

$$
\begin{aligned}
x(t) &:= \begin{bmatrix} g_p(t), & g_t(t), & g_{sc}(t), & i_p(t), & i_l(t), & i_{sc1}, & i_{sc2}, & i_{d1}, & i_{d2} \end{bmatrix}^T \\
y(t) &:= g_{sc}(t), \quad u(t) := \begin{bmatrix} u_{ra}(t) & u_{ins}(t) \end{bmatrix}^T \\
\tilde{u}(t) &:= \begin{bmatrix} k_{p1} & u_{ii}(t) & u_{iir}(t) \end{bmatrix}^T.
\end{aligned}
$$

The matrices A_c, $B_{c,1}$, $B_{c,2}$ and C_c are shown in Equation (7) where $B_{c,1}$ is defined to be the first two columns of B_c while $B_{c,2}$ as the last three columns of B_c. Here, subcutaneous glucose concentration $g_{sc}(t)$ was considered the output which also represents an uncorrupted measurement of subcutaneous glucose. The equation for u_{egp} was substituted in the equation for g_p. Matrix C can be redefined if more measurements are available, including, for example, multiple CGM

measurements and/or plasma glucose and insulin concentration measurements, if available.

Since CGM measures subcutaneous glucose in discrete form, we may discretize Equation (5) using, for example, zero order hold approximation [20], and add measurement noise to obtain the following discrete form of the model:

$$
\begin{aligned}
x_{k+1} &= Ax_k + B_1 u_k + B_2 \tilde{u}_k, & x(0) &= x_0 \\
y_{k+1} &= Cx_{k+1} + v_{k+1} & k &= 0, \dots N-1,
\end{aligned}
\tag{6}
$$

where $x_k = x(kTs) \in \mathbb{R}^9_+$, $y_k = y(kT_s) \in \mathbb{R}_+$, $u_k = u(kT_s) \in \mathbb{R}^2_+$, $\tilde{u}_k = \tilde{u}(kT_s) \in \mathbb{R}^3_+$, where N is the number of CGM measurements. The additional sequence $v_{k+1} \in \mathbb{R}$ in Equation (6) is an unknown sequence and may account for any deviation from the linear relationship in Equation (6), including, for example, measurement noise. CGM measurement noise has been studied in [21] by comparing CGM recordings with plasma glucose concentration measurements and was modeled as a random sequence using a Johnson distribution with autoregressive dynamics. This model will be used to generate the noise sequence in the simulation study.

Assumption 2.2. *The model parameters for the patient, represented in matrix A_c, are known.*

Techniques for identifying patient model parameters for the UVa Padova model using triple tracer measurements are described in [7] and using plasma glucose and insulin concentration measurements are described in [22].

3 PROBLEM FORMULATION

The objective of this study is to estimate the glucose flux disturbances u_{ra}, u_{egp} and u_{ins} during a meal using (1) noisy CGM measurements; (2) insulin infusion recordings; (3) patient model parameters for the transport model described earlier; (4) an estimate of the initial state vector $\bar{x}_0$ (5) an estimate of the amount of meal carbohydrates in the meal being consumed $\bar{c}_{carbs}(\mathrm{mg})$ and (6) and a sparse vector space representing the space of plausible glucose flux profiles for each flux type. A constrained Lasso formulation will be used to estimate these fluxes which is developed next.

3.1 Constrained Lasso Formulation
We first expand the input output sequence relationship given by Equation (6) in matrix form as follows:

$$
Y_N = \Theta_N x_0 + T_{N_1} U_N + T_{N_2} \tilde{U}_N + V_N
\tag{8}
$$

where $Y_N := \begin{bmatrix} y_1 \\ \vdots \\ y_N \end{bmatrix}$, $U_N := \begin{bmatrix} u_0 \\ \vdots \\ u_{N-1} \end{bmatrix}$, $\tilde{U}_N := \begin{bmatrix} \tilde{u}_0 \\ \vdots \\ \tilde{u}_{N-1} \end{bmatrix}$

$$
V_N := \begin{bmatrix} v_1 \\ \vdots \\ v_N \end{bmatrix}, \quad \Theta_N := \begin{bmatrix} CA \\ CA^2 \\ \vdots \\ CA^N \end{bmatrix}
$$

$$
T_{N_i} := \begin{bmatrix} CB_i & 0 & \cdots & 0 \\ CAB_i & CB_i & \ddots & 0 \\ \vdots & & \ddots & 0 \\ CA^{N-1}B_i & CA^{N-2}B_i & \cdots & CB_i \end{bmatrix}, \quad i = 1, 2.
$$

Assumption 3.1. *The discrete state matrix A is marginally stable; i.e., $|eig(A)| \leq 1$. Marginal stability also requires that the geometric multiplicity of the eigenvalues on the unit circle to be not larger than 1. Furthermore, we assume that the matrix formed by the first n block rows of Θ_N, denoted by Θ_n, is full column rank.*

Assumption (3.1) is needed so that the term $\Theta_N x_0$ is bounded; i.e., the sequence $CA^s x_0$ converges to a bounded solution as $s \to \infty$. The other part of the assumption is needed for guaranteeing a unique estimate of x_0 using the output sequence y_k and both the input sequences u_k and $\tilde{u}_k$ in finite time, which is known as the observability condition in system theory.

We define the glucose flux profile vectors as follows:

$$
U_{ra} := [u_{ra}(0), \dots, u_{ra}((N-1)T_s)]^T
$$
$$
U_{ins} := [u_{ins}(0), \dots, u_{ins}((N-1)T_s)]^T.
$$

Assumption 3.2. *The glucose flux profiles U_{ra} and U_{ins} live inside a low dimensional subspace of the space spanned by the column vectors of the dictionary matrices $D_{ra} \in \mathbb{R}^{N \times p_{ra}}$ and $D_{ins} \in \mathbb{R}^{N \times p_{ins}}$, respectively; i.e:*

$$
U_{ra} = D_{ra}\alpha_{ra}, \quad U_{ins} = D_{ins}\alpha_{ins},
$$

where $\alpha_{ra} \in \mathbb{R}^{p_{ra}}$ and $\alpha_{ins} \in \mathbb{R}^{p_{ins}}$ are sparse vectors with $|\alpha_{ra}| = s_{ra}$ and $|\alpha_{ins}| = s_{ins}$.

The construction of the sparse dictionaries D_{ra} and D_{ins} using dictionary learning will be discussed later in Section 4. Consequently, we may express the input vector U_N as follows:

$$
A_c := \begin{bmatrix}
-(k_1+k_{p2}) & k_2 & 0 & 0 & 0 & 0 & 0 & -k_{p3} & 0 \\
k_1 & -k_2 & 0 & 0 & 0 & 0 & 0 & 0 & 0 \\
1/(\tau v_g) & 0 & -1/\tau & 0 & 0 & 0 & 0 & 0 & 0 \\
0 & 0 & 0 & -(m_2+m_4) & m_1 & k_{a1} & k_{a2} & 0 & 0 \\
0 & 0 & 0 & m_2 & -(m_1+m_3) & 0 & 0 & 0 & 0 \\
0 & 0 & 0 & 0 & 0 & -(k_d+k_{a1}) & 0 & 0 & 0 \\
0 & 0 & 0 & 0 & 0 & k_d & -k_{a2} & 0 & 0 \\
0 & 0 & 0 & 0 & 0 & 0 & 0 & -k_i & k_i \\
0 & 0 & 0 & k_i/v_i & 0 & 0 & 0 & 0 & -k_i
\end{bmatrix}, \quad
B_c := \begin{bmatrix}
1 & 0 & 1 & -1 & 0 \\
0 & -1 & 0 & 0 & 0 \\
0 & 0 & 0 & 0 & 0 \\
0 & 0 & 0 & 0 & 0 \\
0 & 0 & 0 & 0 & 0 \\
0 & 0 & 0 & 0 & 1 \\
0 & 0 & 0 & 0 & 0 \\
0 & 0 & 0 & 0 & 0 \\
0 & 0 & 0 & 0 & 0
\end{bmatrix}
\tag{7}
$$

$$
C_c := [0 \quad 0 \quad 1 \quad 0 \quad 0 \quad 0 \quad 0 \quad 0 \quad 0], \; B_c = [B_{c,1} \; B_{c,2}], \; B_{c,1}(:, 1:2), \; B_{c,2} = B_c(:, 3:5)
$$

$$U_N = D_N \boldsymbol{\alpha}, \qquad (9)$$

where

$$D_N := \begin{bmatrix} d_{ra,1}^T & 0 \\ 0 & d_{ins,1}^T \\ d_{ra,2}^T & 0 \\ 0 & d_{ins,2}^T \\ \vdots & \vdots \\ d_{ra,N}^T & 0 \\ 0 & d_{ins,N}^T \end{bmatrix}, \quad \boldsymbol{\alpha} := \begin{bmatrix} \alpha_{ra} \\ \alpha_{ins} \end{bmatrix}. \qquad (10)$$

Here, $d_{ra,1}, d_{ra,2}, \dots d_{ra,N} \in \mathbb{R}^{p_{ra}}$ are the N row vectors of D_{ra}, and $d_{ins,1}, d_{ins,2}, \dots d_{ins,N}$ are the N row vectors of D_{ins}, respectively. As a result, we can rewrite (8) as:

$$Y_N = \Theta_N x_0 + \Phi \boldsymbol{\alpha} + T_{N_2} \tilde{U}_N + V_N \qquad (11)$$
$$\text{where } \Phi = T_{N_1} D_N.$$

Using the set membership framework of estimation [23], we introduce additional a priori information on x_0 as an ℓ_2 norm bound constraint given by:

$$\|x_0 - \bar{x}_0\|_2 \leq \epsilon_{x_0}, \qquad (12)$$

where $\bar{x}_0$ is an estimate of the initial state vector and ϵ_{x_0} is a known upper bound on the ℓ_2 norm error for this estimate. Assuming steady state basal conditions are established at time zero, a plausible value for $\bar{x}_0$ could be: [18]

$$\bar{x}_0 = [\bar{g}_{p,0}, \ \bar{g}_{t,0}, \ \bar{g}_{sc,0}, \ \bar{i}_{p,0}, \ \bar{i}_{l,0}, \ \bar{i}_{sc1,0}, \ \bar{i}_{sc2,0}, \ \bar{i}_{d1,0}, \ \bar{i}_{d2,0}]^T$$
$$\bar{g}_{p,0} = v_g \hat{g}_0, \quad \bar{g}_{t,0} = \frac{k_1}{k_2} v_g \hat{g}_0, \quad \bar{g}_{sc,0} = \hat{g}_0, \quad \bar{i}_{p,0} = \hat{i}_0, \quad \bar{i}_{l,0} = \hat{i}_0$$
$$\bar{i}_{sc1,0} = i_{sc1ss}, \ \bar{i}_{sc2,0} = i_{sc2ss}, \ \bar{i}_{d1,0} = \bar{i}_{d2,0} = \hat{i}_0 / v_i, \qquad (13)$$

where $\hat{g}_0 (\mathrm{mg/dl})$ and $\hat{i}_0$ are plasma glucose and insulin concentration measurement taken at time zero. For the other states, the basal values will be used in the absence of direct measurements. Here, we can also have individual ℓ_2 error bounds for each element of x_0 if necessary to reflect the level of uncertainty for each initial state.

Additional a priori information can be incoporated related to the amount of meal carbohydrates. The area under the curve of $u_{ra}(t)$ represents the amount of glucose absorbed from meal carbohydrates and the following relationship is used [24]:

$$c_{carbs} = \frac{c_{bw}}{f} \int_{t=0}^{t=NT_s} u_{ra}(t)dt \approx \frac{c_{bw}}{f} \cdot \sum_{k=0}^{N} u_{ra}(kT_s)T_s, \qquad (14)$$

where f is the fraction of meal carbohydrates absorbed as glucose in plasma (glucose bioavailability), $c_{bw}(\mathrm{kg})$ the patient body weight and $c_{carbs}(\mathrm{mg})$ amount of meal carbohydrates consumed. In [7], bioavailability was assumed fixed for all patients and given by $f = 0.9$ (i.e., assuming no abnormalities in glucose absorption in the patient is present). In practice, meal carbohydrate measurement c_{carbs} can be subject to uncertainties. We will assume that the uncertainty in c_{carbs} can be represented also as an ℓ_2 norm bound constraint on c_{carbs} as follows:

$$\|c_{carbs} - \bar{c}_{carbs}\|_2 \leq \epsilon_{carbs},$$

where c_{carbs} is defined according to Equation (14), $\bar{c}_{carbs}$ is an initial estimate of meal carbohydrates and ϵ_{carbs} reflects the level of uncertainty in this measurement.

Consequently, estimating the glucose fluxes amounts to the estimation of initial state vector x_0 and the sparse vector $\boldsymbol{\alpha}$. The following convex program is proposed for estimating both x_0 and $\boldsymbol{\alpha}$:

$$\boldsymbol{\alpha}^*, x_0^* = arg \min_{\boldsymbol{\alpha}, x_0 \succeq 0} \|Y_N - \Theta_N x_0 - T_{N_2} \tilde{U}_N - T_{N_1} D_N \boldsymbol{\alpha}\|_2^2 + \lambda \|\boldsymbol{\alpha}\|_1$$

subject to:
$$\|x_0 - \bar{x}_0\|_2 \leq \epsilon_{x_0}, \quad \|c_{carbs} - \bar{c}_{carbs}\|_2 \leq \epsilon_{carbs}$$
$$D_{ra}\alpha_{ra} \succeq 0, \quad D_{ins}\alpha_{ins} \succeq 0.$$
$$(15)$$

We mention the following related to the proposed convex program:

1) The ℓ_2 norm term in the minimization ensures that the estimated vectors x_0^* and $\boldsymbol{\alpha}^*$ are consistent with the noisy CGM measurements in the least squares sense.
2) The ℓ_1 norm term in the minimization ensures that the estimated vector $\boldsymbol{\alpha}^*$ is sparse following Assumption 3.2.
3) Using the set membership framework of estimation [23], the ℓ_2 norm bound constraints on x_0 and c_{carbs} will limit the solution space of x_0 and c_{carbs} to the ℓ_2 norm balls defined by the centers $\bar{x}_0$, $\bar{c}_{carbs}$ and the radii ϵ_{x_0}, ϵ_{carbs}, respectively.
4) Finally, the positivity constraints $D_{ra}\alpha_{ra} \succeq 0$ and $D_{ins}\alpha_{ins} \succeq 0$ are imposed to limit to positive glucose flux profiles for u_{ra} and u_{ins}, respectively. On the other hand, the positivity constraint $\alpha \succeq 0$ is used if non-negative sparse encoding of the glucose fluxes is used (explained later in Section 4).

The above formulation can be related to non-negative Lasso estimation that is known for its support recovery properties and robustness to nonlinear distrotions [25]. A suitable value for the parameter λ can be found by repeated solution of Equation (15) over a range of values arranged lograthimcally starting with a small value $\lambda \approx 0$ to a value that results into having $\boldsymbol{\alpha} = 0$ [19]. Consequently, the value of λ that results into having the most plausible shape for the glucose fluxes is then selected. Finally we mention that the convex program Equation (15) can be solved using, for example, interior point solvers as discussed in [26].

After solving Equation (15), the glucose flux profiles can then be found from the individual flux dictionaries as follows:

$$\begin{bmatrix} U_{ra}^* \\ U_{ins}^* \end{bmatrix} = \begin{bmatrix} D_{ra} & 0 \\ 0 & D_{ins} \end{bmatrix} \alpha^*. \qquad (16)$$

If desired, estimates of the unknown state sequence x_k for $k = 1, \dots, N$ can also be found by solving the following recursion:

$$x_k^* = A^k x_0^* + \sum_{j=0}^{k-1} A^{k-j-1} \Big(B_1 u_j^* + B_2 \tilde{u}_j \Big), \quad k = 1, \dots N, \qquad (17)$$

where $u_j^* = [u_{ra}^*(T_s j), \ u_{ins}^*(T_s j)] = [d_{ra,j}^T \alpha_{ra}^*, \ d_{ins,j}^T \alpha_{ins}^*]$. Finally, estimation of the sequence $u_{egp}(kT_s)$ is found from the following recursion:
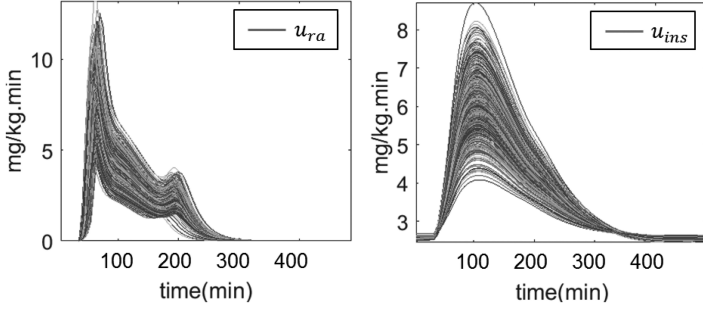
Fig. 2. A subset of the data generated using the UVa/Padova simulator [18] for the average adult patient. Left: data set for u_{ra} and right: data set for u_{ins}.

$$u_{egp}(kT_s)^* = k_{p1} - k_{p2}x_{k,1}^* - k_{p3}x_{k,2}^*, \quad k = 1, \ldots N. \quad (18)$$

4 SPARSE ENCODING OF PLAUSIBLE GLUCOSE FLUX PROFILES

Assumption (3.1) requires dictionaries that can express the unknown glucose fluxes using a combination of a small number of basis vectors. Predefined basis vectors, such as wavelets and Fourier basis, are often effective for approximating smooth signals. However, in the estimation of glucose fluxes, there could be an unlimited number of different combinations of smooth signals that are consistent with the transport Equations in (1) and the available glucose measurements. In this study, the distinctive features of the various glucose flux profiles are exploited in the estimation of the unmeasured disturbances by constructing special basis vectors for these signals from an available large training set of plausible glucose flux profiles. As shown in Fig. 2, u_{ra} exhibits a distinctive jump at the start of the meal followed by a slow decay as compared to the profile of u_{ins} that rises and falls at a slower rate during meals. Hence, forming sparse dictionaries (finding the sparse signal building blocks or basis vectors) that can capture and sparsely encode these intrinsic signal characteristics for the glucose fluxes is desirable for reconstructing these signals.

In this study, the FDA approved UVa Padova simulator is used to generate a large number of plausible glucose flux profiles, for a range of patient parameters, which will be used as a training set for constructing sparse basis vectors. The UVa Padova model (version 3.2) is used for simulating 3 average in-silico patients; average adolescent (virtual patient 11); average adult (virtual patient 22) and average child (virtual patient 33) under the same scenario which will be explained next.

The duration of the scenario was set to 208 days with 1 meal every 8 hours and a simulation step size of 1 minute. The time of bolus insulin injection was set to be 1 minute before the start of each meal to mimic the meal tolerance test protocols given in [13]. The amount of CHOs in each meal and the duration of each meal was randomized using Matlab's normally distributed random number generator to generate rich data. The amount of CHOs was set with a mean of 50 grams and a variance of 10 grams per meal. The duration of each meal was set with a mean of 15 minutes and a variance of 5 minutes per meal while ensuring no meal duration exceeds 30 minutes. The amount of bolus insulin delivered was calculated based on the formula given in [18]

(Equation (15)) which uses patient CIR and a correction factor. The correction factor is found using the so-called 1700 rule (Equation (16) in [18]).

The basal insulin injection rate was fixed and set to the patient specific rate which corresponds to the rate required to maintain fasting levels. Also, the value of u_{ii} was set constant to $u_{ii} = u_{cns} = 1$ mg/kg/min and glucose bioavailability was set to $f = 0.9$ in all experiments. The total number of meal flux profiles for all 3 average in-silico patients was 1875. Afterwards, each meal flux profile was segmented to 480 minutes in duration. Fig. 2 shows samples of the generated flux profiles for the average adult in-silico patient.

The sparse encoding problem can be described as follows: given a set of n_{ra} training vectors for U_{ra}; i.e., $U_{ra}^1, \ldots, U_{ra}^{n_{ra}}$ and n_i training vectors for U_{ins}; i.e., $U_{ins}^1, \ldots, U_{ins}^{n_{ins}}$ find matrices D_{ra} and D_{ins} that satisfy the following [27]:

$$\min_{D_{ra}\in\mathscr{C},\,\alpha_{ra}\succeq0} \sum_{i=1}^{n_{ra}}\left(\frac{1}{2}\|U_{ra}^i - D_{ra}\alpha_{ra}^i\|_2^2 + \gamma\|\alpha_{ra}^i\|_1\right)$$

$$\min_{D_{ins}\in\mathscr{C},\,\alpha_{ins}\succeq0} \sum_{i=1}^{n_i}\left(\frac{1}{2}\|U_{ins}^i - D_{ins}\alpha_{ins}^i\|_2^2 + \gamma\|\alpha_{ins}^i\|_1\right),$$

(19)

where the set $\mathscr{C}$ is given by:

$$\mathscr{C} \triangleq \left\{D \in \mathbb{R}^{N\times p_{ra}} : \|d_j\|_2 \leq 1, \quad \forall j\right\},$$

where $D \in \{D_{ra}, D_{ins}\}$, while d_j is the jth column vector of D_{ra} or D_{ins}. The dictionaries, D_{ra} and D_{ins} are constrained to the set $\mathscr{C}$ to avoid having vectors with large numbers. For the case when p_{ra}, $p_{ins} > N$ an over-complete dictionary with non-orthogonal vectors will result. Positivity constraints on α_{ra} and α_{ins} were used for convenience only so that the codes are plotted as positive numbers and to make the results more interpretive. Generally, it is desirable to reduce the number of basis vectors as much as possible to have a more compact representation of the vector space, which can ultimately help in enhancing the recovery conditions of Lasso estimates [19]. On the other hand, reducing the number of basis vectors, will increase the error between the training set vectors and the corresponding sparse representation of the vector space. The tuning parameter γ is selected for setting a desired sparsity level on $\boldsymbol{\alpha}_{ra}$ and $\boldsymbol{\alpha}_{ins}$ and can also reflect our confidence in the training set signals U_{ra}^i and U_{ins}^i. Problem Equation (19) is a non-convex optimization problem that can be locally solved (i.e., for stationary points). Most algorithms use convex programming and alternate in solving for the dictionary and the codes while applying some update until convergence is obtained or maximum number of iterations is reached. In this study, the online dictionary algorithm developed in [28] is used. The parameters of the on-line dictionary learning algorithm (Algorithm 14 in [27]) were set to the following: $\gamma = 0.1$; $T_{num} = 3000$; $N = 97$; $p_{ra} = p_{ins} = 50$ and $n_{ra} = n_{ins} = 625$.

A validation set was generated by simulating 30 different in-silico patient parameter sets provided by the UVa Padova simulator. The parameter sets numbered from 1 to 33 (skipping patients 11, 22 and 33 that were used in developing D_{ra} and D_{ins}) for the adolescent, the adult and the child virtual patients were used. Each virtual patient has a unique parameter set that reflects, for example, a unique level of insulin sensitivity. The same meal tolerance test conditions described earlier was then used but with a different random sequence

TABLE 2
Relative Root Mean Square Error Performance, Average Cardinality $avg(|\alpha_i^*|)$, and Average ℓ_1 Norm of α_i^* for Flux Dictionaries D_{ra} and D_{ins} Using 30 Different Model Parameter Sets

Dictionary	$RRMSE_{D,avg}$	$avg(|\alpha_i^*|)$	$avg(\|\alpha_i^*\|_1)$
D_{ra}	0.05	4	33.8
D_{ins}	0.09	2.9	44.4

TABLE 3
Relative Root Mean Square Error, Average Cardinality $avg(|\alpha_i^*|)$, and Average ℓ_1 Norm of α_i^* for Flux Dictionaries $\tilde{D}_{ra}$ and $\tilde{D}_{ins}$ Using 30 Different Model Parameter Sets

Dictionary	$RRMSE_{D,avg}$	$avg(|\alpha_i^*|)$	$avg(\|\alpha_i^*\|_1)$
$\tilde{D}_{ra}$	0.071	6.0	92.2
$\tilde{D}_{ins}$	0.0493	3.9	60.3

for the amount of meal CHOs and the duration for each meal. Consequently, a total of 18750 flux profiles per flux type were generated to form the validation set. The following Lasso problem was then solved:

$$\alpha_{ra}^{i*} = arg \min_{\alpha_{ra}^i \succeq 0} \frac{1}{2}\|U_{ra}^i - D_{ra}\alpha_{ra}^i\|_2^2 + \gamma\|\alpha_{ra}^i\|_1$$
$$\alpha_{ins}^{j*} = arg \min_{\alpha_{ins}^j \succeq 0} \frac{1}{2}\|U_{ins}^j - D_{ins}\alpha_{ins}^j\|_2^2 + \gamma\|\alpha_{ins}^j\|_1, \tag{20}$$

where $i = 1,\ldots,n_{ra}$, $j = 1,\ldots,n_{ins}$ and $\gamma = 0.1$. The average relative root mean square error $RRMSE_{D,avg}$ was calculated as follows:

$$RRMSE_{D,avg} = \frac{1}{n \cdot U_{range}} \sum_{i=1}^{n} \frac{1}{\sqrt{N}}\|U_i - D\alpha^{i*}\|_2,$$

where D is either D_{ra} or D_{ins}; n is either n_{ra} or n_{ins}; U_i is either U_{ra}^i or U_{ins}^i and α^{i*} is either α_{ra}^{i*} or α_{ins}^{i*}. Here, U_{range} is $U_{max} - U_{min}$ and is equal to 14 for U_{ra} and 8.7 for U_{ins}. The average cardinality of all sparse codes $|\alpha_{ra}^{i*}|$ and $|\alpha_{ins}^{i*}|$ was also found by counting the average number of non-zero elements all flux profiles. Table 2 shows the $RRMSE_{D,avg}$ and average cardinality for the corresponding sparse codes for each flux dictionary obtained. The performance measures indicate that the basis vectors constructed for the glucose flux profiles can sparsely represent a large set of glucose flux profiles beyond the training set.

4.1 Multiple Insulin Injections and Meal Stages

The simulation experiments for constructing D_{ra} and D_{ins} were limited to the case when steady state basal conditions are established prior to the meal and when a single bolus insulin injection is made just one minute before the start of a single meal. This scenario mimics the conditions of a clinical meal tolerance test. However, there could be numerous variations from this scenario in a real life setting. For example, multiple bolus insulin injections may be delivered during a single meal. These injections may be taken before the meal, during the meal or after the meal. Also, the meal itself may be consumed at multiple stages with intermediate resting periods. The sparse encoding process explained earlier can be extended to such cases when plausible glucose flux profiles for these different meal scenarios are available. However, there could be an unlimited number of plausible glucose flux profiles for these various scenarios that may not be easy to generate and to make available for the dictionary learning process. Hence, the following assumption is made.

Assumption 4.1. *Given that $\tilde{U}_{ra} \in \mathbb{R}^N$ is the glucose rate of appearance profile for a meal consumed at $r_m \in \mathbb{I}$ different stages in time and $\tilde{U}_{ins} \in \mathbb{R}^N$ is the insulin dependent glucose*

utilization profile for a meal with $r_i \in \mathbb{I}$ insulin injections, then $\tilde{U}_{ra}$ and $\tilde{U}_{ins}$ live inside a low dimensional subspace of the space spanned by the column vectors of the dictionary matrices $\tilde{D}_{ra} \in \mathbb{R}^{N\times(r_m \times p_{ra})}$ and $\tilde{D}_{ins} \in \mathbb{R}^{N\times(r_i \times p_{ins})}$ given by:

$$\tilde{D}_{ra} = [D_{ra}^1 \quad D_{ra}^2 \quad \cdots D_{ra}^{r_m}]$$
$$\tilde{D}_{ins} = [D_{ins}^1 \quad D_{ins}^2 \quad \cdots D_{ins}^{r_i}], \tag{21}$$

where D_{ra}^i, $i = 1,2,\ldots,r_m$ are circularly shifted versions of D_{ra} corresponding to r_m meal stages and D_{ins}^i, $i = 1,2,\ldots,r_i$ are circularly shifted versions of D_{ins} corresponding to r_i insulin injections respectively.

Circular shifting of dictionary basis vectors can be done by multiplying each vector with an appropriate permutation matrix that circularly shifts each column vector in D_{ra} and D_{ins}. To demonstrate the validity of this assumption, we have simulated 200 meals for 30 in-silico patients (total 6000 meals) using the UVA/Padova simulator under a scenario that contains two meal insulin boluses and two meal stages shifted randomly in time. The total insulin bolus for both meals was calculated using patient CIR (as explained above) and meal carbohydrates and was split into two equal boluses delivered before and after the first meal with random time shifts. The random time shifts were generated using Matlab's random number generator with zero mean and variance of 30 minutes from the starting time of the first meal stage. Similarly, the second meal was initiated with random time shifts from the first meal stage.

Consequently, two time shifted versions of D_{ra} (i.e., D_{ra}^1 and D_{ra}^2) and D_{ins} (i.e., D_{ins}^1 and D_{ins}^2) were formed using the first and second meal stage times and first and second bolus insulin injection times, respectively. The performance of the combined matrices; i.e., $\tilde{D}_{ra}$, $\tilde{D}_{ins}$, was tested by solving Equation (20) for each glucose flux signal profile U_{ra} and U_{ins} with $\lambda = 0.5$. Table 3 shows the $RRMSE_D$, average cardinality and average ℓ_1 norm value for all sparse codes for each dictionary. The low RRMSE values indicate that the basis vectors constructed for the glucose flux profiles for single meals can be also used to represent glucose flux profiles for multiple meals and insulin injections. Fig. 3 shows a sample of the results obtained.

5 SIMULATION STUDY

The performance of the proposed estimator will now be tested for three in-silico patients for two different scenarios. The first set of experiments validate performance under meal tolerance test conditions assuming model parameters, time of meals, time of insulin injections are known with certainty. The second set of simulation experiments will validate performance when two meal stages and two bolus insulin injections are present.
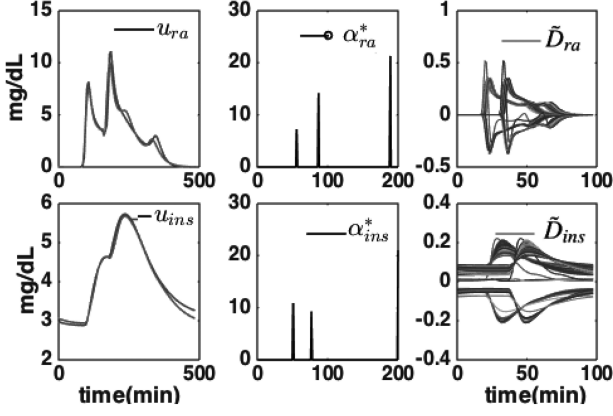
Fig. 3. Left plots: original signals u_{ra}, u_{ins} and corresponding sparse coded signals $u_{ra}^* = \tilde{D}_{ra}\alpha_{ra}^*$, $u_{ins}^* = \tilde{D}_{ins}\alpha_{ins}^*$ for in-silico patient number 10. Middle plots: The corresponding elements of the sparse vectors α_{ra}^* and α_{ins}^*; Right plots: The matrices $\tilde{D}_{ra}$ and $\tilde{D}_{gu}$ used.

5.1 Scenario 1: Meal Tolerance Test Conditions

In this set of experiments, subcutaneous glucose measurements were first generated using the UVa Padova simulator under the MTT scenario explained earlier in Section 4. Three in-silico patients were simulated; namely the average adolescent, average adult and average child patient as before. The model parameters for the in-silico patients are shown in Table 4 and assumed known. A total of 100 meal profiles were generated for testing with random amounts of meal CHOs and meal durations as explained earlier in Section 4 but with a different random seed to generate a validation set. The simulation resulted in forming all state signals for each meal and for each patient (i.e., $x(t)$ for each experiment).

Three sets of continuous time system matrices A_c, B_c, C_c (one for each patient) were then formed using patient parameters given in Table 4 according to the definition given in Equation (7). The continuous system matrices were then discretized using zero order hold approximation with $T_s = 5$ min to obtained matrices A, B and C needed to construct the discrete time system Equation (6) for each patient. The magnitude of the eigenvalues of A were found to be strictly less than 1 and Θ_n to be of rank 9 and hence Assumption 3.1 holds.

For each meal and for each patient, the measurement vector sequence was constructed as $y_k = g_{sc}(kT_s) + v_k$, where $v_k \in \mathbb{R}$ is generated using a SU Johnson distribution with an autoregressive dynamic as explained in [21]. Using the notation given in [21], the parameters of the SU Johnson are: $\tilde{\lambda} = 15.96$, $\tilde{\gamma} = -0.5444$, $\delta = 1.69$, $\tilde{\xi} = -5.47$ and the autocorrelation coefficient $\tilde{\kappa} = 0.7$. The initial estimate for the state was set to $\bar{x}_0 = x_0 + \tilde{v}$, where x_0 is the true value of the state at time zero and $\tilde{v} \in \mathbb{R}^9$ is additive normally distributed pseudo-random noise vector generated in Matlab with zero mean and covariance matrix $5 \times I_9$. Similarly, $c_{carbs} = \bar{c}_{carbs} + \tilde{v}$, where $\bar{c}_{carbs}$ is the value used in the simulation experiment and $\tilde{v}$ is additive normally distributed noise with zero mean and covariance of 1. The known input sequence $\tilde{u}_k$ was set to $\tilde{u}_k = [k_{p1}, u_{cns}, u_{iir}(kT_s)]^T$ using the same bolus and basal insulin inputs used in simulation. The other parameters in Equation (15) were set as follows: $\epsilon_{x_0} = 5$, $\lambda = 0.1$, $f = 0.9$. Finally, the glucose flux dictionaries D_{ra} and D_{ins} constructed in Section 4 for the MTT conditions were used.

Consequently, the minimization problem Equation (15) was solved using Matlab CVX [29] for the average adolescent, average adult and average child patient respectively for all 100 trials. Fig. 4 shows a sample of the results obtained for

TABLE 4
Patient Parameters for Averge Adolescent, Average Adult, and Average Child in-silico Patients [7]

Patient/Param.	avg. adolescent	avg. adult	avg. child
k_1(min^{-1})	0.0870	0.0731	0.0746
k_2(min^{-1})	0.0902	0.1077	0.1050
v_g(dl/kg)	1.8354	1.8480	1.8313
m_1(min^{-1})	0.2135	0.1850	0.1889
m_2(min^{-1})	0.3026	0.3130	0.2648
m_3(min^{-1})	0.3202	0.2775	0.2833
m_4(min^{-1})	0.1211	0.1252	0.1059
v_i(l/kg)	0.0503	0.0511	0.0480
k_{a1}(min^{-1})	0.0038	0.0038	0.0043
k_{a2}(min^{-1})	0.0176	0.0177	0.0197
k_d(min^{-1})	0.0168	0.0162	0.0168
k_{p1}(mg/kg min)	5.4807	4.9866	5.0789
k_{p2}(min^{-1})	0.0048	0.0055	0.0049
k_{p3}(mgl/kg min pmol)	0.0136	0.0105	0.0098
k_i(min^{-1})	0.0100	0.0109	0.0101
c_{bw}(kg)	48.77	69.6	29.97
f	0.9	0.9	0.9
τ(min^{-1})	11	11	11
i_{pb}(pmole/kg)	5.45	5.42	5.09
i_{lb}(pmole/kg)	3.09	3.67	2.85
i_{sc1ss}(pmole/kg)	79.95	84.79	63.84
i_{sc2ss}(pmole/kg)	76.35	77.57	54.29

this simulation experiment. As it can be observed in the figure, good estimation results were achieved for all glucose flux types and for all three in-silico patients despite the noise present in CGM measurements, the initial conditions and the meal information provided. Moreover, these results were achieved despite using the same set of flux dictionaries for all patients. Estimation performance was measured using average relative root mean square error for all estimated signals given by:

$$RRMSE = \frac{1}{N_e \cdot X_{range}} \sum_{i=1}^{N_e} \frac{1}{\sqrt{N}} \|X_i^* - X_i\|_2,$$

where X_i is either u_{ra}, u_{egp}, u_{ins}, or g; X_i^* is either $u_{ra}^*, u_{egp}^*, u_{ins}^*$ or g, the corresponding estimated signal vectors; $X_{range} = \max_i X_i - \min_i X_i$; $N_e = 100$ the total number of meals under analysis and N the size of the signal vector. Table 5 provides the relative average root mean square error values obtained for the three in-silico patients under study for all the simulation runs. Note, that g^* is the simulated plasma glucose profile using the estimated profiles u_{ra}^*, u_{egp}^* and u_{ins}^* and can be obtained recursively using Equation (17). The low relative root mean square error values demonstrate good recovery of all glucose fluxes which demonstrates the potential of the technique when patient parameters are known. Good estimation results were also found for the states x_k^* that were found by solving Equation (17) and the estimated initial condition x_0^* (results not shown due to limited space).

5.2 Scenario 2: Two Meal Stages and Bolus Injections

In the following simulation experiment, the scenario when two meal stages and/or two bolus injections are present will be examined. Simulation data was first generated using the UVA Padova simulator, as before, using the same simulation
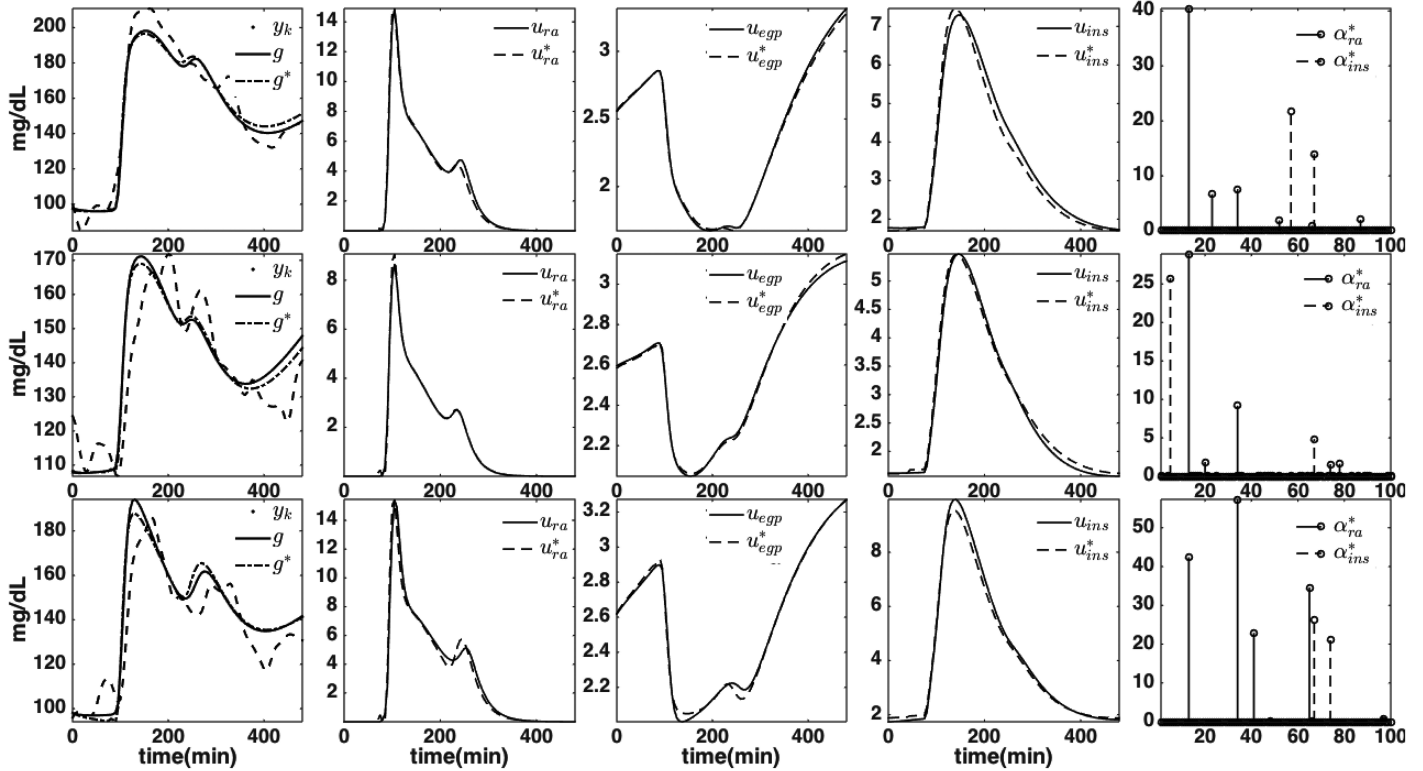
Fig. 4. Example of the results obtained for scenario 1. The top block row of plots are (from left) g mg/dl, u_{ra}, u_{egp}, and u_{ins} in mg/kg min and the corresponding estimated values g^*, u_{ra}^*, u_{egp}^*, u_{ins}^*, and α_{ra}^*, α_{ins}^* for the average adolescent patient. The second block row of plots is the same simulated for the average adult patient and the third block row of plots is for the average child patient.

details explained earlier in scenario 1 but with two meals and two bolus injections at random occurrence times. All remaining simulation details are identical to what was discussed in scenario 1.

To accommodate for the two meals and two bolus insulin injections, two time shifted versions of D_{ra} and D_{ins} were formed (i.e., D_{ra}^1, D_{ra}^2 and D_{ins}^1, D_{ins}^2) according to the known meal occurance and known insulin injection times. The union of the two dictionaries formed $\tilde{D}_{ra}$ and $\tilde{D}_{ins}$ according to Equation (21). Consequently, the minimization problem Equation (15) was solved using Matlab CVX [29] for the average adolescent, average adult and average child patient respectively for one single trial. The result of this experiment is shown in Fig. 5. As it can be observed in the figure, overall good estimation results for the glucose fluxes was achieved compared with their true values, with some bias errors originating possibly from the approximation that was used. This experiment demonstrates the possibility of extending the technique to multiple meals and multiple insulin injection scenarios using the same basis vectors constructed for single meal/ single insulin injection scenarios.

6 EXPERIMENTAL STUDY

Validation against the gold standard triple tracer technique developed in [9] will be considered here, which requires triple tracer measurements to be collected simultaneously with CGM measurements and insulin infusion recordings for the patients. Experiments appearing in [30] satisfy this criteria and data was shared with us and obtained from the UVa Center for Diabetes Technology. The triple tracer measurements obtained were intravenous plasma glucose g, glucose rate of appearance u_{ra}, endogenous glucose production u_{egp}, insulin dependent glucose utilization u_{ins} and plasma insulin concentration i for 3 T1DM patients undergoing the triple tracer protocol as explained in [30]. Also included are subcutaneous CGM measurements y, measured every 5 minutes using a CGM device coupled to the patient; the amount and time of bolus and basal insulin administered to the patient that is used to form the input signal u_{iir}, and the amount of meal CHOs consumed in every meal c_{carbs} for single meal tests lasting 480 minutes each. Detail information about each patient, the meal being analyzed, amount of insulin administered to the patient and the time of bolus insulin injections is shown in Table 6. The body weight and the triple tracer measurements are in terms of fat free mass (FFM). For more details about the meals consumed, patient parameters and experimental setup the reader is refered to [30]. No ethical approval for anonymous collection of retrospective patient data is needed.

Since patient model parameters are unknown in this study, nor could we identify patient model parameters from another experiment, we only demonstrate here that there exist a certain selection of model parameters that can be used in our technique for reproducing the triple tracer measurements and for estimating the missing measurements.

Consequently, our method given by the solution of Equation (15) was implemented for each 480 minute meal

TABLE 5
Average Relative Root Mean Square Error Performance
for Estimated Values u_{ra}^*, u_{egp}^*, u_{ins}^*, and g^* for
100 Random Simulation Trials (Scenario 1)

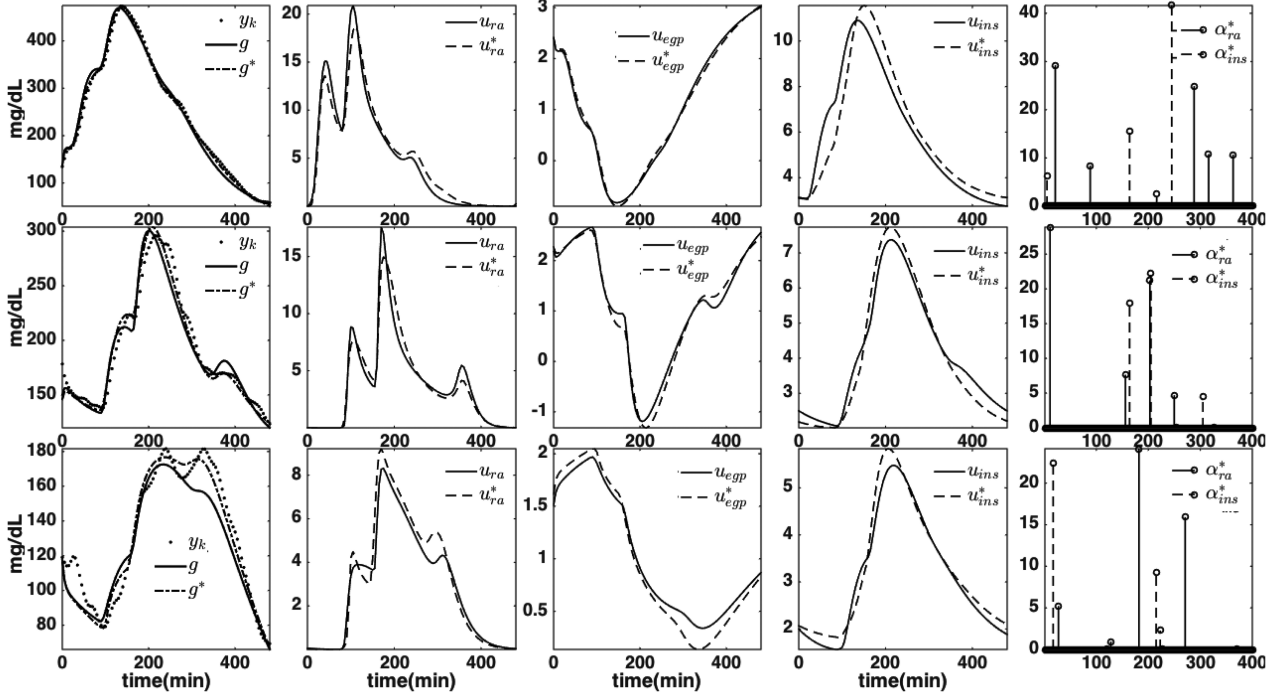| Patient/$RRMSE$	u_{ra}^*	u_{egp}^*	u_{ins}^*	g^*
average adolescent	0.0347	0.2070	0.0505	0.0512
average adult	0.0403	0.2600	0.0527	0.0643
average child	0.0308	0.1401	0.0304	0.0415
Average	0.0353	0.202	0.0405	0.0523

Fig. 5. Results obtained for scenario 2. The top block row of plots are (from left) g mg/dl, u_{ra}, u_{egp}, and u_{ins} in mg/kg min and the corresponding estimated values g^*, u_{ra}^*, u_{egp}^*, u_{ins}^*, and α_{ra}^*, α_{ins}^* for the average adolescent patient. The second block row of plots is the same simulated for the average adult patient and the third block row of plots is for the average child patient.

TABLE 6
Patient and Meal Information

Patient #	Age	c_{bw}(kg) (FFM)	c_{carbs}(g)	Premeal Bolus 1, 2, 3 (U)	Time 1, 2, 3(min)	Meal Bolus (U)	Time 4 (min)	Avg. Basal Rate (U/hr)
1	58	63.9	50.4	1.0, 0.5, -	-84, -54, -	4	-4	0.405
2	19	41.7	47.6	3.0, 1.5, 2	-175, -115, -55	5	-5	0.66
3	22	46.2	52.2	0.9, -, -	-155, -, -	5.9	0	1.35

experiment. Patient parameters were first selected from the UVa Padova library using a simple search technique that finds the parameter set that gives the smallest value of the objective function in Equation (15). Adjustments to these parameters were then made manually and the parameters used after these adjustments are shown in Table 7. On the other hand, the initial condition of the state x_0 was set using the given initial measured values of plasma glucose $g(0)$ and initial plasma insulin $i(0)$ according to Equation (13). To reflect our uncertainty in the initial state and meal carbohydrates we set $\epsilon_{x_0} = 10$ and $\epsilon_{carbs} = 10$. Multiple time shifted versions of the flux dictionary D_{ins} were formed corresponding to the multiple insulin injection times using the techniques discussed earlier in Section 4. The value of the tuning parameter λ was selected using trial and error and is shown in Table 8.

Fig. 6 show plots of the estimated fluxes using both the triple tracer technique (black dots) and the new technique (dash lines) for each patient. Table 8 gives the RRMSE for the estimated fluxes and the estimated signals g^* and i^*. In view of the results, the following are some observations regarding the validity of the technique proposed:

1) The relatively low RRMSE values for the estimated signals shown in Table 8 indicate that the method is capable of reproducing the triple tracer measurements with good accuracy in all three experiments. The discrepancy between the two techniques (particularly for

patient 3) can be attributed to parameter uncertainties; sensor calibration errors and measurement noise.

2) The plausibility of the shape of the glucose flux profiles; particularly the shape of u_{ins}^* in relation to the time and magnitude of the bolus insulin injections is

TABLE 7
Patient Parameters Used in the Experimental Study

Patient/Param.	Patient #1	Patient #2	Patient #3
k_1(min^{-1})	0.0136	0.1931	0.0710
k_2(min^{-1})	0.0224	0.1083	0.0895
v_g(dl/kg)	2.59	1.3629	1.3291
m_1(min^{-1})	0.3282	0.1317	0.3282
m_2(min^{-1})	0.2759	0.4593	0.2759
m_3(min^{-1})	0.4923	0.1976	0.7384
m_4(min^{-1})	0.1103	0.1837	0.1103
v_i(l/kg)	0.1044	0.0516	0.0685
k_{a1}(min^{-1})	0.0042	0.0030	0.0017
k_{a2}(min^{-1})	0.0132	0.0114	0.0069
k_d(min^{-1})	0.0196	0.0055	0.0196
k_{p1}(mg/kg min)	10.44	11.49	5.70
k_{p2}(min^{-1})	0.008	0.0140	0.0060
k_{p3}(mgl/kg min pmol)	0.0475	0.0272	0.0119
k_i(min^{-1})	0.0140	0.0102	0.0364
c_{bw}(kg)	63.9	41.7	46.2
f	0.9	0.9	0.9
τ(min^{-1})	14.3	21.67	3.57
i_{pb}(pmole/kg)	4.35	8.39	8.85
i_{lb}(pmole/kg)	1.46	11.7	2.29
i_{sc1ss}(pmole/kg)	86.99	167.85	176.99
i_{sc2ss}(pmole/kg)	86.99	167.85	176.99

TABLE 8
Tuning and Estimation Performance for Experimental Study

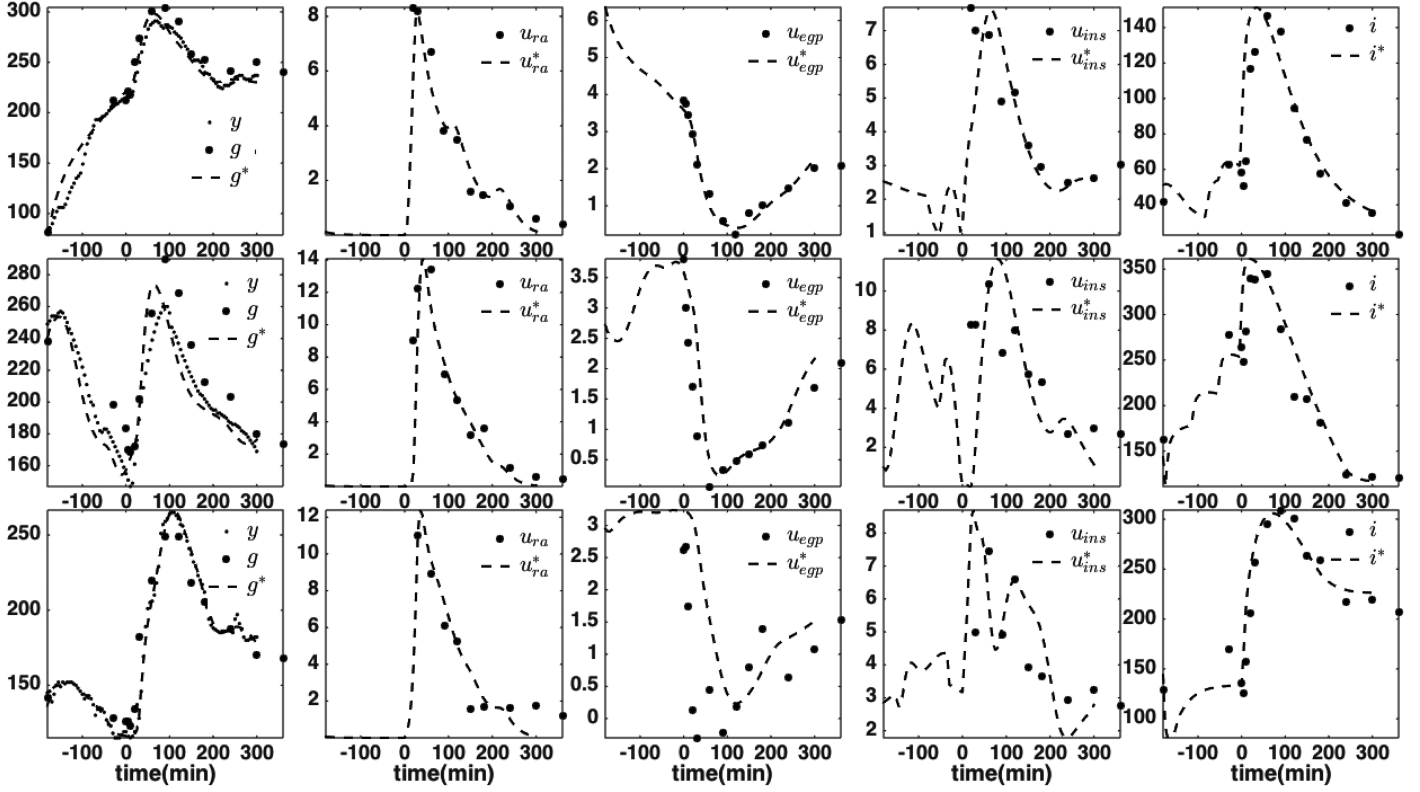| Patient #	λ	RRMSE for y^*	RRMSE for g^*	RRMSE for i^*	RRMSE for u_{ra}^*	RRMSE for u_{egp}^*	RRMSE for u_{ins}^*
1	0.01	0.47	0.309	1.037	0.060	0.040	0.123
2	0.01	0.6	0.771	1.029	0.106	0.105	0.296
3	0.001	0.46	0.590	0.740	0.101	0.289	0.211

Fig. 6. Results obtained for Patient 1 (top row), Patient 2 (middle row), and Patient 3 (bottom row).

evident in all three experiments. In other words, the technique gives plausible estimates of u_{ins}^* that reflect the relative effect of the bolus insulin injections made before the meal.

We emphasize here that in all three experiments the same original set of matrices D_{ra} and D_{ins} (before time shifting) were used, demonstrating the main hypothesis of this study.

7 DISCUSSION AND CONCLUSION

A new technique for estimating plasma glucose fluxes has been introduced. The approach uses a transport model for each patient combined with a sparse vector space that encodes the space of plausible glucose flux profiles. The technique was tested in simulation demonstrating near recovery of glucose fluxes even under complex CGM noise and when multiple insulin injections and meal stages are present. Other important state variables can be estimated, including plasma glucose and plasma insulin concentrations provided that patient parameters are known in advance. The method was tested using experimental data obtained for 3 T1DM patients undergoing the triple tracer meal protocol while connected to CGM devices. The results indicate the validity of the technique for all three patients for a certain selection of patient model parameters.

We note here that the technique is not limited to the model structure given by the UVa Padova model and other model structures can be used to enhance robustness of the technique to parameter uncertainties. Also, the library of plausible glucose flux profiles could be obtained using other techniques; i. e. a database of real triple tracer meal protocol measurements rather than obtained from simulation. The problem of optimally finding a state space representation from limited triple tracer measurements is important for obtaining patient model parameters and for enabling the usage of our technique. In addition, a theoretical study is warranted for validating the method and analyzing the experimental conditions required for good estimation performance in view of Lasso inference theory [19]. Finally, more validation experiments are needed to understand whether the same model parameters can be used for different meals.

REFERENCES

[1] P. Home, "Plasma insulin profiles after subcutaneous injection: How close can we get to physiology in people with diabetes?" *Diabetes, Obesity Metabolism*, vol. 17, no. 11, pp. 1011–1020, 2015.

[2] F. J. Doyle, L. M. Huyett, J. B. Lee, H. C. Zisser, and E. Dassau, "Closed-loop artificial pancreas systems: Engineering the algorithms," *Diabetes Care*, vol. 37, no. 5, pp. 1191–1197, 2014.

[3] Y. C. Kudva, R. E. Carter, C. Cobelli, R. Basu, and A. Basu, "Closed-loop artificial pancreas systems: Physiological input to enhance next-generation devices," *Diabetes Care*, vol. 37, no. 5, pp. 1184–1190, 2014.

[4] X. Peng, Y. Tang, W. He, W. Du, and F. Qian, "A just-in-time learning based monitoring and classification method for hyper/hypocalcemia diagnosis," *IEEE/ACM Trans. Comput. Biol. Bioinf.*, vol. 15, no. 3, pp. 788–801, May/Jun. 2017.

[5] C. Dalla Man, M. Camilleri, and C. Cobelli, "A system model of oral glucose absorption: Validation on gold standard data," *IEEE Trans. Biomed. Eng.*, vol. 53, no. 12, pp. 2472–2478, Dec. 2006.

[6] P. A. Smeets, A. Erkner, and C. De Graaf, "Cephalic phase responses and appetite," *Nutrition Rev.*, vol. 68, no. 11, pp. 643–655, 2010.

[7] C. D. Man, R. A. Rizza, and C. Cobelli, "Meal simulation model of the glucose-insulin system," *IEEE Trans. Biomed. Eng.*, vol. 54, no. 10, pp. 1740–1749, Oct. 2007.

[8] R. A. Rizza, G. Toffolo, and C. Cobelli, "Accurate measurement of postprandial glucose turnover: Why is it difficult and how can it be done (relatively) simply?" *Diabetes*, vol. 65, no. 5, pp. 1133–1145, 2016.

[9] R. Basu, B. Di Camillo, G. Toffolo, A. Basu, P. Shah, A. Vella, R. Rizza, and C. Cobelli, "Use of a novel triple-tracer approach to assess postprandial glucose metabolism," *Amer. J. Physiology-Endocrinology Metabolism*, vol. 284, no. 1, pp. E55–E69, 2003.

[10] R. Steele, "Influences of glucose loading and of injected insulin on hepatic glucose output," *Ann. New York Acad. Sci.*, vol. 82, no. 2, pp. 420–430, 1959.

[11] A. Mari, "Estimation of the rate of appearance in the non-steady state with a two-compartment model," *Amer. J. Physiology-Endocrinology Metabolism*, vol. 263, no. 2, pp. E400–E415, 1992.

[12] R. Hovorka, H. Jayatillake, E. Rogatsky, V. Tomuta, T. Hovorka, and D. T. Stein, "Calculating glucose fluxes during meal tolerance test: A new computational approach," *Amer. J. Physiology-Endocrinology Metabolism*, vol. 293, no. 2, pp. E610–E619, 2007.

[13] A. Haidar, E. Potocka, B. Boulet, A. M. Umpleby, and R. Hovorka, "Estimating postprandial glucose fluxes using hierarchical bayes modelling," *Comput. Methods Programs Biomedicine*, vol. 108, no. 1, pp. 102–112, 2012.

[14] P. Herrero, J. Bondia, C. C. Palerm, J. Vehí, P. Georgiou, N. Oliver, and C. Toumazou, "A simple robust method for estimating the glucose rate of appearance from mixed meals," *J. Diabetes Sci. Technol.*, vol. 6, no. 1, pp. 153–162, 2012.

[15] R. N. Bergman, "The minimal model of glucose regulation: A biography," in *Mathematical Modeling in Nutrition and the Health Sciences*. New York, NY, USA: Springer, 2003, pp. 1–19.

[16] F. Cameron, G. Niemeyer, and B. A. Buckingham, "Probabilistic evolving meal detection and estimation of meal total glucose appearance," *J. Diabetes Sci.Technol.*, vol. 3, no. 5, pp. 1022–1030, 2009.

[17] C. Novara, N. M. Pour, T. Vincent, and G. Grassi, "A nonlinear blind identification approach to modeling of diabetic patients," *IEEE Trans. Control Syst. Technol.*, vol. 24, no. 3, pp. 1092–1100, May 2016.

[18] C. Dalla Man, F. Micheletto, D. Lv, M. Breton, B. Kovatchev, and C. Cobelli, "The uva/padova type 1 diabetes simulator new features," *J. Diabetes Sci. Technol.*, vol. 8, no. 1, pp. 26–34, 2014.

[19] T. Hastie, R. Tibshirani, and M. Wainwright, *Statistical Learning with Sparsity: The Lasso and Generalizations*. Boca Raton, FL, USA: CRC Press, 2015.

[20] C. Rabbath and N. Léchevin, *Discrete-Time Control System Design with Applications*. New York, NY, USA: Springer, 2013. [Online]. Available: https://books.google.com.sa/books?id=Ai-8BAAAQBAJ

[21] M. Breton and B. Kovatchev, "Analysis, modeling, and simulation of the accuracy of continuous glucose sensors," *J. Diabetes Sci. Technol.*, vol. 2, no. 5, pp. 853–862, 2008.

[22] R. Visentin, C. Dalla Man, and C. Cobelli, "One-day bayesian cloning of type 1 diabetes subjects: Toward a single-day uva/padova type 1 diabetes simulator," *IEEE Trans. Biomed. Eng.*, vol. 63, no. 11, pp. 2416–2424, Nov. 2016.

[23] M. Milanese and A. Vicino, "Optimal estimation theory for dynamic systems with set membership uncertainty: An overview," *Automatica*, vol. 27, no. 6, pp. 997–1009, 1991.

[24] C. Della Man, A. Caumo, and C. Cobelli, "The oral glucose minimal model: Estimation of insulin sensitivity from a meal test," *IEEE Trans. Biomed. Eng.*, vol. 49, no. 5, pp. 419–429, May 2002.

[25] Y. Itoh, M. F. Duarte, and M. Parente, "Perfect recovery conditions for non-negative sparse modeling," *IEEE Trans. Signal Process.*, vol. 65, no. 1, pp. 69–80, Jan. 2017.

[26] S. P. Boyd and L. Vandenberghe, *Convex Optimization*. Cambridge, U.K.: Cambridge Univ. Press, 2004.

[27] J. Mairal, F. Bach, J. Ponce, and G. Sapiro, "Online dictionary learning for sparse coding," in *Proc. 26th Annu. Int. Conf. Mach. Learn.*, New York, NY, USA: ACM, 2009, pp. 689–696.

[28] J. Mairal, F. Bach, and J. Ponce, "Sparse modeling for image and vision processing," *arXiv:1411.3230*, 2014.

[29] M. Grant and S. Boyd, "CVX: Matlab software for disciplined convex programming, version 2.0 beta," Sep. 2012. [Online]. Available: http://cvxr.com/cvx

[30] L. Hinshaw, C. Dalla Man, D. K. Nandy, A. Saad, A. E. Bharucha, J. A. Levine, R. A. Rizza, R. Basu, R. E. Carter, C. Cobelli, et al., "Diurnal pattern of insulin action in type 1 diabetes: Implications for a closed loop system," *Diabetes*, vol. 62, pp. 2223–2229, 2013.